Search for Invisible Decays of η and η' in $J/\psi \to \phi\eta$ and $\phi\eta'$

M. Ablikim,[1] J. Z. Bai,[1] Y. Ban,[12] J. G. Bian,[1] X. Cai,[1] H. F. Chen,[17] H. S. Chen,[1] H. X. Chen,[1] J. C. Chen,[1] Jin Chen,[1]
Y. B. Chen,[1] S. P. Chi,[2] Y. P. Chu,[1] X. Z. Cui,[1] Y. S. Dai,[19] L. Y. Diao,[9] Z. Y. Deng,[1] Q. F. Dong,[15] S. X. Du,[1] J. Fang,[1]
S. S. Fang,[2] C. D. Fu,[1] C. S. Gao,[1] Y. N. Gao,[15] S. D. Gu,[1] Y. T. Gu,[4] Y. N. Guo,[1] Y. Q. Guo,[1] Z. J. Guo,[16] F. A. Harris,[16]
K. L. He,[1] M. He,[13] Y. K. Heng,[1] H. M. Hu,[1] T. Hu,[1] G. S. Huang,[1,*] X. T. Huang,[13] X. B. Ji,[1] X. S. Jiang,[1] X. Y. Jiang,[5]
J. B. Jiao,[13] D. P. Jin,[1] S. Jin,[1] Yi Jin,[8] Y. F. Lai,[1] G. Li,[2] H. B. Li,[1] H. H. Li,[1] J. Li,[1] R. Y. Li,[1] S. M. Li,[1] W. D. Li,[1] W. G. Li,[1]
X. L. Li,[1] X. N. Li,[1] X. Q. Li,[11] Y. L. Li,[4] Y. F. Liang,[14] H. B. Liao,[1] B. J. Liu,[1] C. X. Liu,[1] F. Liu,[6] Fang Liu,[1] H. H. Liu,[1]
H. M. Liu,[1] J. Liu,[12] J. B. Liu,[1] J. P. Liu,[18] Q. Liu,[1] R. G. Liu,[1] Z. A. Liu,[1] Y. C. Lou,[5] F. Lu,[1] G. R. Lu,[5] J. G. Lu,[1]
C. L. Luo,[10] F. C. Ma,[9] H. L. Ma,[1] L. L. Ma,[1] Q. M. Ma,[1] X. B. Ma,[5] Z. P. Mao,[1] X. H. Mo,[1] J. Nie,[1] S. L. Olsen,[16]
H. P. Peng,[17,§] R. G. Ping,[1] N. D. Qi,[1] H. Qin,[1] J. F. Qiu,[1] Z. Y. Ren,[1] G. Rong,[1] L. Y. Shan,[1] L. Shang,[1] C. P. Shen,[1]
D. L. Shen,[1] X. Y. Shen,[1] H. Y. Sheng,[1] H. S. Sun,[1] J. F. Sun,[1] S. S. Sun,[1] Y. Z. Sun,[1] Z. J. Sun,[1] Z. Q. Tan,[4] X. Tang,[1]
G. L. Tong,[1] G. S. Varner,[16] D. Y. Wang,[1] L. Wang,[1] L. L. Wang,[1] L. S. Wang,[1] M. Wang,[1] P. Wang,[1] P. L. Wang,[1]
W. F. Wang,[1,†] Y. F. Wang,[1] Z. Wang,[1] Z. Y. Wang,[1] Zhe Wang,[1] Zheng Wang,[2] C. L. Wei,[1] D. H. Wei,[1] N. Wu,[1] X. M. Xia,[1]
X. X. Xie,[1] G. F. Xu,[1] X. P. Xu,[6] Y. Xu,[11] M. L. Yan,[17] H. X. Yang,[1] Y. X. Yang,[3] M. H. Ye,[2] Y. X. Ye,[17] Z. Y. Yi,[1] G. W. Yu,[1]
C. Z. Yuan,[1] J. M. Yuan,[1] Y. Yuan,[1] S. L. Zang,[1] Y. Zeng,[7] Yu Zeng,[1] B. X. Zhang,[1] B. Y. Zhang,[1] C. C. Zhang,[1]
D. H. Zhang,[1] H. Q. Zhang,[1] H. Y. Zhang,[1] J. W. Zhang,[1] J. Y. Zhang,[1] S. H. Zhang,[1] X. M. Zhang,[1] X. Y. Zhang,[13]
Yiyun Zhang,[14] Z. P. Zhang,[17] D. X. Zhao,[1] J. W. Zhao,[1] M. G. Zhao,[1] P. P. Zhao,[1] W. R. Zhao,[1] Z. G. Zhao,[1,‡]
H. Q. Zheng,[12] J. P. Zheng,[1] Z. P. Zheng,[1] L. Zhou,[1] N. F. Zhou,[1,‡] K. J. Zhu,[1] Q. M. Zhu,[1] Y. C. Zhu,[1] Y. S. Zhu,[1]
Yingchun Zhu,[1,§] Z. A. Zhu,[1] B. A. Zhuang,[1] X. A. Zhuang,[1] and B. S. Zou[1]

(BES Collaboration)

[1]*Institute of High Energy Physics, Beijing 100049, People's Republic of China*
[2]*China Center for Advanced Science and Technology (CCAST), Beijing 100080, People's Republic of China*
[3]*Guangxi Normal University, Guilin 541004, People's Republic of China*
[4]*Guangxi University, Nanning 530004, People's Republic of China*
[5]*Henan Normal University, Xinxiang 453002, People's Republic of China*
[6]*Huazhong Normal University, Wuhan 430079, People's Republic of China*
[7]*Hunan University, Changsha 410082, People's Republic of China*
[8]*Jinan University, Jinan 250022, People's Republic of China*
[9]*Liaoning University, Shenyang 110036, People's Republic of China*
[10]*Nanjing Normal University, Nanjing 210097, People's Republic of China*
[11]*Nankai University, Tianjin 300071, People's Republic of China*
[12]*Peking University, Beijing 100871, People's Republic of China*
[13]*Shandong University, Jinan 250100, People's Republic of China*
[14]*Sichuan University, Chengdu 610064, People's Republic of China*
[15]*Tsinghua University, Beijing 100084, People's Republic of China*
[16]*University of Hawaii, Honolulu, Hawaii 96822, USA*
[17]*University of Science and Technology of China, Hefei 230026, People's Republic of China*
[18]*Wuhan University, Wuhan 430072, People's Republic of China*
[19]*Zhejiang University, Hangzhou 310028, People's Republic of China*
(Received 4 July 2006; published 16 November 2006)

Using a data sample of 58×10^6 J/ψ decays collected with the Beijing Spectrometer II detector at the Beijing Electron Positron Collider, searches for invisible decays of η and η' in J/ψ to $\phi\eta$ and $\phi\eta'$ are performed. The ϕ signals, which are reconstructed in K^+K^- final states, are used to tag the η and η' decays. No signals are found for the invisible decays of either η or η', and upper limits at the 90% confidence level are determined to be 1.65×10^{-3} for the ratio $\frac{B(\eta \to \text{invisible})}{B(\eta \to \gamma\gamma)}$ and 6.69×10^{-2} for $\frac{B(\eta' \to \text{invisible})}{B(\eta' \to \gamma\gamma)}$. These are the first searches for η and η' decays into invisible final states.

Invisible decays of quarkonium states such as J/ψ and Υ, etc., offer a window into what may lie beyond the standard model (SM) [1,2]. The reason is that, apart from neutrinos, the standard model includes no other invisible final particles into which these states can decay. It is such a window that we intend to further explore by presenting

here the first experimental limits on invisible decays of η and η', which complement the limit of 2.7×10^{-7} recently established in Ref. [3] for the invisible decays of $\pi°$.

Theories beyond the SM generally include new physics, such as, possibly, light dark matter (LDM) particles [4]. These can have the right relic abundance to constitute the nonbaryonic dark matter of the Universe, if they are coupled to the SM through a new light gauge boson U [5] or exchanges of heavy fermions. It is also possible to consider a light neutralino with coupling to the SM mediated by a light scalar singlet in the next-to-minimal supersymmetric standard model [6].

Recently, observations of a bright 511 keV γ-ray line from the galactic bulge have been reported by the SPI spectrometer on the International Gamma-Ray Astrophysics Laboratory (INTEGRAL) satellite [7]. The corresponding galactic positron flux, as well as the smooth symmetric morphology of the 511 keV emission, may be interpreted as originating from the annihilation of LDM particles into e^+e^- pairs [4] (also constrained by Ref. [8]). It is in any case very interesting to search for such light invisible particles in collider experiments. CLEO gave an upper bound on $Y(1S) \rightarrow \gamma + \text{invisible}$, which is sensitive to dark matter candidates lighter than about 3 GeV/c^2 [9] and also provides an upper limit on the axial coupling of the new U boson to the b quark. It is crucial, in addition, to search for the invisible decays of light quarkonium ($q\bar{q}$, $q = u$, d, or s quark) states which can be used to constrain the masses of LDM particles and the couplings of the new boson to the light quarks [2]. We present here measurements of branching fractions of η and η' decays into invisible final states.

The data used in this analysis, consisting of 58×10^6 J/ψ events, were accumulated with the Beijing Spectrometer II (BES II) detector [10], at the Beijing Electron Positron Collider (BEPC). BES II is a conventional solenoidal magnetic detector that is described in detail in Ref. [10]. A 12-layer vertex chamber (VC) surrounding the beam pipe provides trigger and coordinate information. A 40-layer main drift chamber (MDC), located radially outside the VC, provides trajectory and energy loss (dE/dx) information for charged tracks over 85% of the total solid angle. The momentum resolution is $\sigma_p/p = 0.017\sqrt{1 + p^2}$ (p in GeV/c), and the dE/dx resolution for hadron tracks is ~8%. An array of 48 scintillation counters surrounding the MDC measures the time of flight (TOF) of charged tracks with a resolution of ~200 ps for hadrons. Radially outside the TOF system is a 12 radiation length, lead-gas barrel shower counter (BSC). This measures the energies of electrons and photons over ~80% of the total solid angle with an energy resolution of $\sigma_E/E = 22\%/\sqrt{E}$ (E in GeV). Outside of the solenoid coil, which provides a 0.4 T magnetic field over the tracking volume, is an iron flux return that is instrumented with three double layers of counters that identify muons with momentum greater than 0.5 GeV/c.

In order to detect invisible η and η' decays, we use $J/\psi \rightarrow \phi\eta$ and $\phi\eta'$ decays. These two-body decays provide a very simple event topology, as shown in Fig. 1, in which the ϕ signals can be reconstructed easily and cleanly decaying into K^+K^-. The reconstructed ϕ particles can be used to tag η and η' in order to allow a search for their invisible decays. Since both ϕ and η (η') have narrow widths, which are negligible compared with the detector resolution, the shape of the momentum distribution of ϕ is approximately Gaussian. The mean value of the ϕ momentum distribution is 1.320 GeV/c for $J/\psi \rightarrow \phi\eta$ and 1.192 GeV/c for $J/\psi \rightarrow \phi\eta'$. The missing momentum $P_{\text{miss}} = |\vec{P}_{\text{miss}}|$ is a powerful discriminating variable to separate signal events from possible backgrounds, in which the missing side is not from η (η') decay. Here $\vec{P}_{\text{miss}} = -\vec{P}_\phi$. The η and η' signal regions are defined as $|P_{\text{miss}} - 1.320| < 3\sigma_{\text{reso}}^\eta$ for $J/\psi \rightarrow \phi\eta$ and $|P_{\text{miss}} - 1.192| < 3\sigma_{\text{reso}}^{\eta'}$ for $J/\psi \rightarrow \phi\eta'$, where $\sigma_{\text{reso}}^\eta$ (22 MeV/c) and $\sigma_{\text{reso}}^{\eta'}$ (20 MeV/c) are detector resolutions of P_{miss} for $J/\psi \rightarrow \phi\eta$ and $J/\psi \rightarrow \phi\eta'$, respectively. In addition, the η and η' decay regions are easy to define in the lab system due to the strong boost of the ϕ from J/ψ decay, as shown in Fig. 1.

In the event selection, the total number of charged tracks is required to be two with net charge zero. Each track should have a good helix fit in the MDC, and the polar angle θ must satisfy $|\cos\theta| < 0.8$. The event must originate near the collision point; tracks must satisfy $\sqrt{x^2 + y^2} \leq 2$ cm, $|z| \leq 20$ cm, where x, y, and z are the space coordinates of the point of closest approach of tracks to the beam axis. Particle identification (PID) is performed using combined TOF and dE/dx information, and both charged tracks must be identified as kaons.

We require that events have no other charged tracks besides those of the $\phi \rightarrow K^+K^-$ candidate. We count the number of BSC clusters that could be from a K_L^0 or a photon, N_{BSC}, and require that N_{BSC} be zero in the region outside cones of 30° around the charged kaon tracks. These requirements reject most η and η' decays into visible final states. They also eliminate most backgrounds from multibody decays of $J/\psi \rightarrow \phi + \text{anything}$. In order to ensure that η and η' decay particles are inside the fiducial volume
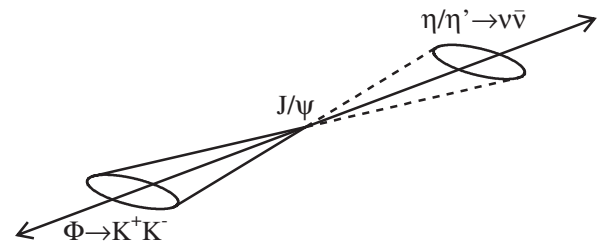
FIG. 1.   Schematic of $J/\psi \rightarrow \phi\eta$ or $\phi\eta'$. The ϕ, which is reconstructed in K^+K^- final states, can be used to tag the invisible decay of η and η'.

of the detector, the recoil direction against ϕ is required to be within the region $|\cos\theta_{\text{recoil}}| < 0.7$, where θ_{recoil} is the polar angle of $\vec{P}_{\text{miss}}$. Figure 2(a) shows the invariant mass distribution of K^+K^- candidates, m_{KK}, after the above selection. A clear ϕ peak is seen. Figure 2(b) shows the P_{miss} distribution for events with $1.005 < m_{KK} < 1.035$ GeV/c^2.

We use Monte Carlo (MC) simulated events to determine selection efficiencies for the signal channels and study possible backgrounds. We obtain efficiencies of 23.5% and 23.2% for η and η' invisible decays, respectively. More than 20 exclusive decay modes are studied with full MC simulations in order to understand the backgrounds. The sources of backgrounds are divided into two classes. Class I: The background is from $J/\psi \to \phi\eta(\eta')$, where $\phi \to K^+K^-$ and $\eta(\eta')$ decays into other modes than the invisible final states. We find that the expected number of background events from this class is negligible for both η and η'. Class II: It is mainly from J/ψ decays to the final states without η or η', such as $\phi K_L K_L$, $\phi f_0(980)(f_0(980) \to K_L K_L)$, and $K^{\star 0} K_L (K^{\star 0} \to K^\pm \pi^\mp)$. For the η case, the dominated background is from the decay of $J/\psi \to K^{\star 0} K_L (K^{\star 0} \to K^\pm \pi^\mp)$, while for the η' case, the dominated background is from the decays of $J/\psi \to \phi K_L K_L$ and $\phi f_0(980)(f_0(980) \to K_L K_L)$. The expected number of background events from class II is 3.0 ± 0.2 and 90 ± 64 in the signal regions for η and η', respectively.

An unbinned extended maximum likelihood (ML) fit is used to extract the event yield for $J/\psi \to \phi\eta(\eta')$ [$\phi \to K^+K^-$ and $\eta(\eta') \to$ invisible]. In the ML fit, we require that $1.00 < P_{\text{miss}} < 1.45$ GeV/c, shown in Fig. 2(b), where the background shape is well understood. We construct probability density functions (PDFs) for the P_{miss} distributions for signals ($\mathcal{F}^\eta_{\text{sig}}$ and $\mathcal{F}^{\eta'}_{\text{sig}}$) and background ($\mathcal{F}_{\text{bkgd}}$) using detailed simulations of signal and background. The PDFs for signals are parametrized by double
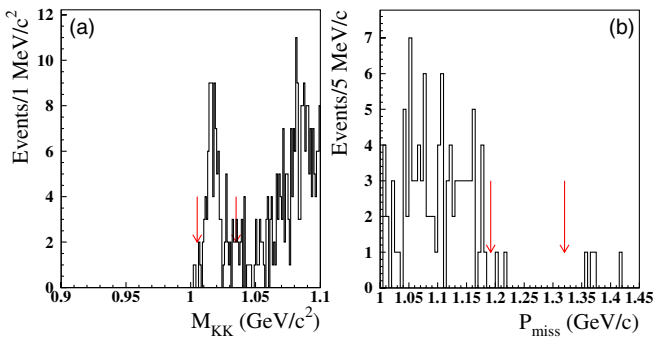
Gaussian distributions with common means, one relative fraction and two distinct widths, which are all fixed to the MC simulation. The PDF for background is a bifurcated Gaussian plus a first order polynomial (P_1). All parameters related to the background shape are floated in the fit to data. The PDFs for signals and background are combined in the likelihood function $\mathcal{L}$, defined as a function of the free parameters N^η_{sig}, $N^{\eta'}_{\text{sig}}$, and N_{bkgd}:

$$
\begin{aligned}
\mathcal{L}(N^\eta_{\text{sig}}, N^{\eta'}_{\text{sig}}, N_{\text{bkgd}}) &= \frac{e^{-(N^\eta_{\text{sig}} + N^{\eta'}_{\text{sig}} + N_{\text{bkgd}})}}{N!} \\
&\times \prod_{i=1}^{N} [N^\eta_{\text{sig}} \mathcal{F}^\eta_{\text{sig}}(P^i_{\text{miss}}) \\
&+ N^{\eta'}_{\text{sig}} \mathcal{F}^{\eta'}_{\text{sig}}(P^i_{\text{miss}}) \\
&+ N_{\text{bkgd}} \mathcal{F}_{\text{bkgd}}(P^i_{\text{miss}})], \quad (1)
\end{aligned}
$$

where N^η_{sig} and $N^{\eta'}_{\text{sig}}$ are the number of $J/\psi \to \phi(\to K^+K^-)\eta(\to \text{invisible})$ and $J/\psi \to \phi(\to K^+K^-)\eta'(\to \text{invisible})$ signal events; N_{bkgd} is the number of background events. The fixed parameter N is the total number of selected events in the fit region, and P^i_{miss} is the value of P_{miss} for the ith event. The negative log-likelihood ($-\ln\mathcal{L}$) is then minimized with respect to N^η_{sig}, $N^{\eta'}_{\text{sig}}$, and N_{bkgd} in the data sample. A total of 105 events is used in the fit, and the resulting fitted values of N^η_{sig}, $N^{\eta'}_{\text{sig}}$, and N_{bkgd} are -2.8 ± 1.4, 2.2 ± 3.4, and 106 ± 11, respectively, where the errors are statistical. Figure 3 shows the P_{miss} distribution and fitted result. No significant signal is observed for the invisible decay of either η or η'. We obtain upper limits by integrating the normalized likelihood distribution over the positive values of the number of signal events. The upper limits at the 90% confidence level are 3.56 events for η and 5.72 events for η', respectively.

FIG. 2 (color online). (a) The m_{KK} distribution for candidate events. The arrows on the plot indicate the signal region of ϕ candidates. (b) P_{miss} distribution for the events with $1.005 < m_{KK} < 1.035$ GeV/c^2 in (a). The means of the missing momenta for $J/\psi \to \phi\eta$ and $J/\psi \to \phi\eta'$ are located around 1.32 and 1.20 GeV/c, respectively, as indicated by the two arrows.
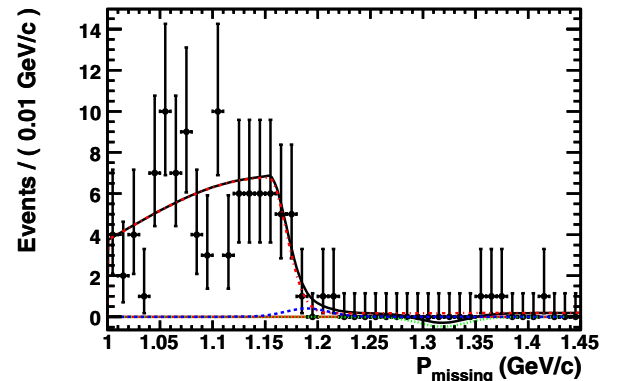

FIG. 3 (color online). The P_{miss} distribution for candidate events. The data (black crosses) are compared to the total fit results. The dotted curve is the projection of η signal component, the dashed curve is the projection of the η' signal component, and the solid curve is the total likelihood fit result.

The branching fraction of $\eta(\eta') \to \gamma\gamma$ is also determined in $J/\psi \to \phi\eta(\eta')$ decays, in order to obtain the ratio of $\mathcal{B}(\eta(\eta') \to \text{invisible})$ to $\mathcal{B}(\eta(\eta') \to \gamma\gamma)$. The advantage of measuring $\frac{\mathcal{B}(\eta(\eta')\to\text{invisible})}{\mathcal{B}(\eta(\eta')\to\gamma\gamma)}$ is that the uncertainties due to the total number of J/ψ events, tracking efficiency, PID, the number of the charged tracks, the cut on m_{KK}, and residual noise in the BSC cancel.

The selection criteria for the charged tracks are the same as those for $J/\psi \to \phi\eta(\eta')$, $\eta(\eta') \to \text{invisible}$ decays. However, at least two good photons are required. A candidate photon must have hits in the BSC. The number of layers hit must be greater than one and the deposited energy in the BSC more than 50 MeV. The angle between the photon emission direction and the shower development direction of the neutral track in BSC is required to be less than 25°. The opening angles between the candidate photons and the charged tracks must be greater than 30°.

The events are kinematically fitted using energy and momentum conservation constraints (4C) under the $J/\psi \to KK\gamma\gamma$ hypothesis in order to obtain better mass resolution and suppress backgrounds further. We require the kinematic fit $\chi^2_{K^+K^-\gamma\gamma}$ less than 50 (15) for the η (η') case. If there are more than two photons, the fit is repeated using all permutations, and the combination with the best fit to $K^+K^-\gamma\gamma$ is retained. The numbers of $J/\psi \to \phi\eta(\eta')$ [$\phi \to K^+K^-$ and $\eta(\eta') \to \gamma\gamma$] events are obtained from fits to the $\gamma\gamma$ invariant mass distributions. The fitted results for $\eta(\eta') \to \gamma\gamma$ are shown in Fig. 4.

Contributions to the systematic error on the ratios are summarized in Table I. Systematic errors in the ML fit originate from the limited number of events in the data sample and from uncertainties in the PDF parametrizations. The uncertainty due to the background shape has been estimated by varying the PDF shape of the background in the ML fit.

The uncertainty, due to the requirement of no neutral clusters in the BSC allowed outside the 30° cones around the charged tracks, is obtained using the control sample of fully reconstructed $J/\psi \to \phi\eta$, $\eta \to \gamma\gamma$ events. The ratios

of events with the requirement on the number of extra photons to events without the requirement are obtained for both data and MC simulation. The difference 5% is considered as the systematic error for both the η and η' cases. This study determines the difference in the noise in the BSC for MC simulation and data. Compared with $\eta \to \text{invisible}$ decay, we expect that more noise is introduced by the photons in $\eta \to \gamma\gamma$ decay. So it is a conservative estimation of the systematic error due to the requirement of no clusters in the BSC for the invisible decays of η and η'.

The uncertainty in the determination of the number of observed $J/\psi \to \phi\eta(\eta')$, $\phi \to K^+K^-$, $\eta(\eta') \to \gamma\gamma$ events is also estimated. Different background shapes are tried in the fit to the $\gamma\gamma$ invariant mass, and the variation of the fitted yields is regarded as a systematic error, which is 2.0% (1.0%) for the η (η') case. The relative systematic error caused by the uncertainty of the photon efficiency is about 4.0% [11]. The uncertainty due to the $\chi^2_{K^+K^-\gamma\gamma}$ constraint is estimated to be 1.0% (5.2%) [12] for the η (η') case. The uncertainty from the trigger efficiency is also considered. The total systematic error $\sigma^{\text{sys}}_{\eta}$ ($\sigma^{\text{sys}}_{\eta'}$) on the ratio is 7.7% (11.1%) for η (η'), as summarized in Table I.

The upper limit on the ratio of $\mathcal{B}(\eta \to \text{invisible})$ to $\mathcal{B}(\eta \to \gamma\gamma)$ is calculated with

$$\frac{\mathcal{B}(\eta \to \text{invisible})}{\mathcal{B}(\eta \to \gamma\gamma)} < \frac{n^{\eta}_{UL}/\epsilon_{\eta}}{n^{\eta}_{\gamma\gamma}/\epsilon^{\eta}_{\gamma\gamma}} \frac{1}{(1-\sigma_{\eta})}, \qquad (2)$$

where n^{η}_{UL} is the 90% upper limit of the number of observed events for $J/\psi \to \phi\eta$, $\phi \to K^+K^-$, $\eta \to \text{invisible}$ decay, ϵ_{η} is the MC determined efficiency for the signal channel, $n^{\eta}_{\gamma\gamma}$ is the number of events for the $J/\psi \to \phi\eta$, $\phi \to K^+K^-$, $\eta \to \gamma\gamma$ decay, $\epsilon^{\eta}_{\gamma\gamma}$ is the MC determined efficiency for the decay mode, and σ_{η} is $\sqrt{(\sigma^{\text{sys}}_{\eta})^2 + (\sigma^{\text{stat}}_{\eta})^2} = 8.1\%$, where $\sigma^{\text{sys}}_{\eta}$ and $\sigma^{\text{stat}}_{\eta}$ are the total relative systematical error for the η case from Table I and the relative statistical error of $n^{\eta}_{\gamma\gamma}$, respectively. For η', $\sigma_{\eta'}$ is $\sqrt{(\sigma^{\text{sys}}_{\eta'})^2 + (\sigma^{\text{stat}}_{\eta'})^2} = 21.6\%$. The relative statistical

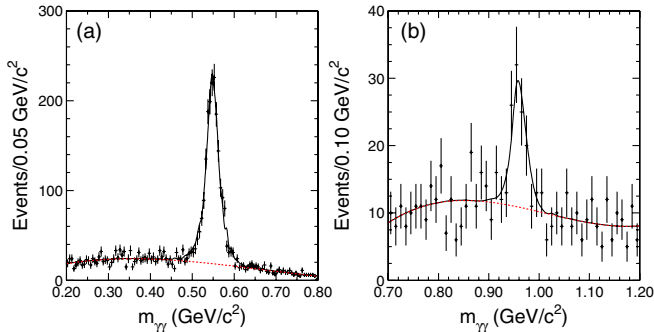

FIG. 4 (color online). (a) The fit of the $\gamma\gamma$ invariant mass distribution of $J/\psi \to \phi\eta$, $\eta \to \gamma\gamma$. The dashed line shows the background, and the solid line is the total fit result. (b) The same plot but for $J/\psi \to \phi\eta'$, $\eta' \to \gamma\gamma$.

TABLE I.　Summary of relative systematic errors. The first three lines are for $J/\psi \to \phi\eta(\eta')$, $\eta(\eta') \to \text{invisible}$. The next three are for $J/\psi \to \phi\eta(\eta')$, $\eta(\eta') \to \gamma\gamma$.

Source of uncertainties	Sys. error (%)	
	η	η'
PDF shapes in the ML fit	3.4	7.3
MC statistics	1.0	1.0
Requirement on N_{BSC}	5.0	5.0
Photon efficiency	4.0	4.0
4C fit for $\eta(\eta') \to \gamma\gamma$	1.0	5.2
Background shape for $\eta(\eta') \to \gamma\gamma$	2.0	1.0
Total	7.7	11.1

TABLE II. The numbers used in the calculations of the ratios in Eq. (2), where $n_{\mathrm{UL}}^{\eta}(n_{\mathrm{UL}}^{\eta'})$ is the upper limit of the signal events at the 90% confidence level, $\epsilon_{\eta}(\epsilon_{\eta'})$ is the selection efficiency, $n_{\gamma\gamma}^{\eta}(n_{\gamma\gamma}^{\eta'})$ is the number of the events of $J/\psi \to \phi\eta(\eta')$, $\phi \to K^{+}K^{-}$, $\eta(\eta') \to \gamma\gamma$, $\epsilon_{\gamma\gamma}^{\eta}(\epsilon_{\gamma\gamma}^{\eta'})$ is its selection efficiency, $\sigma_{\eta}^{\mathrm{stat}}$ ($\sigma_{\eta'}^{\mathrm{stat}}$) is the relative statistical error of $n_{\gamma\gamma}^{\eta}(n_{\gamma\gamma}^{\eta'})$, and $\sigma_{\eta}(\sigma_{\eta'})$ is the total relative error.

Quantity	Value	
	η	η'
n_{UL}^{η} $(n_{\mathrm{UL}}^{\eta'})$	3.56	5.72
ϵ_{η} $(\epsilon_{\eta'})$	23.5%	23.2%
$n_{\gamma\gamma}^{\eta}$ $(n_{\gamma\gamma}^{\eta'})$	1760.2 ± 49.3	71.6 ± 13.2
$\epsilon_{\gamma\gamma}^{\eta}$ $(\epsilon_{\gamma\gamma}^{\eta'})$	17.6%	15.2%
$\sigma_{\eta}^{\mathrm{stat}}$ $(\sigma_{\eta'}^{\mathrm{stat}})$	2.8%	18.5%
σ_{η} $(\sigma_{\eta'})$	8.1%	21.6%

error of the fitted yield for $J/\psi \to \phi\eta(\eta')$, $\eta(\eta') \to \gamma\gamma$, is 2.8% (18.5%) according to the results from the fit to the invariant mass of $\gamma\gamma$ in Fig. 4. We also obtain the upper limit on the ratio of $\mathcal{B}(\eta' \to \text{invisible})$ to $\mathcal{B}(\eta' \to \gamma\gamma)$ by replacing η with η' in Eq. (2). Since only the statistical error is considered when we obtain the 90% upper limit of the number of events, to be conservative, n_{UL}^{η} and $n_{\mathrm{UL}}^{\eta'}$ are shifted up by one sigma of the additional uncertainties (σ_{η} or $\sigma_{\eta'}$).

Using the numbers in Table II, the upper limit on the ratio of $\mathcal{B}(\eta(\eta') \to \text{invisible})$ and $\mathcal{B}(\eta(\eta') \to \gamma\gamma)$ is obtained at the 90% confidence level of 1.65×10^{-3} (6.69×10^{-2}).

In summary, we search for the invisible decay modes of η and η' for the first time in $J/\psi \to \phi\eta(\eta')$ using the 58×10^6 J/ψ events at BES II. We find no signal yields for the invisible decays of η and η' and obtain limits on the ratio $\frac{\mathcal{B}(\eta(\eta') \to \text{invisible})}{\mathcal{B}(\eta(\eta') \to \gamma\gamma)}$. The upper limits at the 90% confidence level are 1.65×10^{-3} and 6.69×10^{-2} for $\frac{\mathcal{B}(\eta \to \text{invisible})}{\mathcal{B}(\eta \to \gamma\gamma)}$ and $\frac{\mathcal{B}(\eta' \to \text{invisible})}{\mathcal{B}(\eta' \to \gamma\gamma)}$, respectively. The advantage of measuring the ratios instead of the branching fractions of the invisible decays is that many uncertainties cancel.

*Present address: Purdue University, West Lafayette, IN 47907, USA.
†Present address: Laboratoire de l'Accélérateur Linéaire, Orsay, F-91898, France.
‡Present address: University of Michigan, Ann Arbor, MI 48109, USA.
§Present address: DESY, D-22607, Hamburg, Germany.

[1] P. Fayet, Phys. Lett. **84B**, 421 (1979); D. Besson *et al.* (CLEO Collaboration), Phys. Rev. D **30**, 1433 (1984); P. Fayet and J. Kaplan, Phys. Lett. B **269**, 213 (1991); B. McElrath, Phys. Rev. D **72**, 103508 (2005).
[2] P. Fayet, Phys. Rev. D **74**, 054034 (2006).
[3] A. V. Artamonov *et al.* (E949 Collaboration), Phys. Rev. D **72**, 091102 (2005).
[4] C. Boehm and P. Fayet, Nucl. Phys. **B683**, 219 (2004); C. Boehm, D. Hooper, J. Silk, M. Casse, and J. Paul, Phys. Rev. Lett. **92**, 101301 (2004); P. Fayet, Phys. Rev. D **70**, 023514 (2004).
[5] P. Fayet, Phys. Lett. **95B**, 285 (1980); P. Fayet, Nucl. Phys. **B187**, 184 (1981).
[6] J. Ellis, J. F. Gunion, H. E. Haber, L. Roszkowski, and F. Zwirner, Phys. Rev. D **39**, 844 (1989); J. F. Gunion, D. Hooper, and B. McElrath, Phys. Rev. D **73**, 015011 (2006).
[7] P. Jean *et al.*, Astron. Astrophys. **407**, L55 (2003); SPI is the spectrometer aboard INTEGRAL.
[8] J. F. Beacom, N. F. Bell, and G. Bertone, Phys. Rev. Lett. **94**, 171301 (2005); P. Fayet, D. Hooper, and G. Sigl, Phys. Rev. Lett. **96**, 211302 (2006).
[9] R. Balest *et al.* (CLEO Collaboration), Phys. Rev. D **51**, 2053 (1995).
[10] J. Z. Bai *et al.* (BES Collaboration), Nucl. Instrum. Methods Phys. Res., Sect. A **344**, 319 (1994).
[11] M. Ablikim *et al.* (BES Collaboration), Phys. Rev. D **71**, 032003 (2005).
[12] J. Z. Bai *et al.* (BES Collaboration), Phys. Rev. D **70**, 012005 (2004).